A renormalisation analysis of the one-dimensional Thue-Morse aperiodic chain

A renormalisation analysis of the one-dimensional Thue–Morse aperiodic chain

Ming-Guang Qin†, Hong-ru Ma‡ and Chien-Hua Tsai‡

† Institute of Condensed Matter Physics, Jiao-Tong University, Shanghai, People's Republic of China
‡ Centre of Theoretical Physics, Chinese Centre of Advanced Science and Technology (World Laboratory), Beijing and Institute of Condensed Matter Physics, Jiao-Tong University, Shanghai, People's Republic of China

Abstract. The one-dimensional Thue–Morse sequence with a generating matrix of determinant 0 has been suggested to be intermediate between a periodic structure and a standard quasi-periodic structure like the Fibonacci sequence. The renormalisation procedure developed in our previous study of the one-dimensional Fibonacci quasi-crystal is applied here to discuss the electronic spectrum of a tight-binding Thue–Morse aperiodic chain. The resulting integrated electronic density of states indeed shows a structure that is more like that of a periodic chain than a Fibonacci quasi-crystal. We suggest that the analytical procedure can be extended to study one-dimensional quasi-crystals of any other kind, the two-dimensional Penrose lattice as well as three-dimensional real quasi-crystals.

1. A tight-binding model of one-dimensional Thue–Morse aperiodic chain

There now exist in the literature a considerable number of theoretical works dealing with the Fibonacci quasi-crystal. But very little attention has been paid to other one-dimensional aperiodic structures. Axel *et al* (1986), Allouche *et al* (1986) and Riklund *et al* (1987) called attention to the Thue–Morse sequence:

LSSLSLLSSLLSLSSL . . .

which has a generating matrix of determinant 0 (Riklund *et al* 1987)

$$\begin{pmatrix} 1 & 1 \\ -1 & -1 \end{pmatrix}.$$

In comparison, the periodic chain

LSLSLSLSLSLSLSLS . . .

has a generating matrix

$$\begin{pmatrix} 1 & 1 \\ 1 & 1 \end{pmatrix}$$

with a null determinant, too, whereas the Fibonacci chain

LSLLSLSLLSLLS . . .

is generated by

$$\begin{pmatrix} 1 & 1 \\ 1 & 0 \end{pmatrix}$$

whose determinant is equal to 1. It is claimed (Riklund *et al* 1987), therefore, that the Thue–Morse structure constitutes a link between a periodic and a Fibonacci chain. Riklund *et al* (1987) solved eigenvalue problems for a number of finite tight-binding Thue–Morse chains to illustrate such a speculation. More recently, Cheng *et al* (1988) published detailed studies of electronic properties of finite Thue–Morse chains in the tight-binding approximation and associated arguments concerning the behaviour of the electronic spectrum in the infinite case.

Niu and Nori (1986) and Ma and Tsai (1988) formulated a renormalisation procedure for the study of the electronic structure of tight-binding Fibonacci quasi-crystals. Combined with the self-similarity in the structure of the Fibonacci sequence, it gives all details in the integrated density of states versus energy behaviour (Ma and Tsai 1988) in complete agreement with a numerical simulation (Ma *et al* 1986). The theory has proved to be useful in the study of quasi-periodic systems (see, for instance, Garg 1988, Appendix B). Here, we apply the same procedure to study the electronic structure of a tight-binding Thue–Morse chain. The results are again satisfactory.

We need, first of all, to formulate more precisely a model for a one-dimensional tight-binding aperiodic chain. The Thue–Morse sequence can also be generated by a very simple rule. Starting with LS, successive substitutions

$$L \to LS \qquad S \to SL \tag{1}$$

give us immediately generations of various order of the sequence:

LS

LSSL

LSSLSLLS   (2)

LSSLSLLSSLLSLSSL

. . ..

Consider now a chain of atoms connected by long (L) and short (S) bonds between nearest neighbours arranged according to the Thue–Morse sequence shown in figure 1.
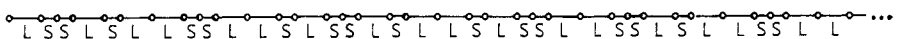

L SS L S L L SS L L S L SS L S L L S L SS L L SS L S L L SS L L ...

Figure 1. A Thue–Morse aperiodic chain consisting of atoms connected by long (L) and short (S) bonds.

We consider the long and short bonds to have unequal strengths, T_L and T_S. Furthermore, each of the atoms must be in any one of three different nearest-neighbour surroundings: (M) connected to other atoms on both sides by long bonds, (D) connected to other atoms on one side by a long bond and on the other side by a short bond and (T) connected to atoms on both sides by short bonds. We consider, in general, atoms in these three different cases to have different single atomic levels e_M, e_D and e_T. Our model is then formulated by the following Hamiltonian:

$$H = \sum_i |i\rangle e_i \langle i| + \sum_{ij} |i\rangle T_{ij} \langle j| \tag{3}$$

where i and j label the atomic sites along the chain and

$$e_i = \begin{cases} e_M & \text{when atom } i \text{ is on an (M) site} \\ e_D & \text{when atom } i \text{ is on a (D) site} \\ e_T & \text{when atom } i \text{ is on a (T) site} \end{cases} \tag{4}$$

$$T_{ij} = \begin{cases} T_L & \text{when } j = i \pm 1 \text{ and the bond between } i \text{ and } j \text{ is a long one} \\ T_S & \text{when } j = i \pm 1 \text{ and the bond between } i \text{ and } j \text{ is a short one} \\ 0 & \text{in any other case.} \end{cases} \tag{5}$$

For simplicity, we discuss in this paper the case of equal atomic levels, and refer all energies to this level, so that $e_M = e_D = e_T = 0$. The stationary Schrödinger equation with Hamiltonian (3) is then

$$T_{i-1,i} |i - 1\rangle + T_{i,i+1} |i + 1\rangle = E|i\rangle \tag{6}$$

E being the electronic energy eigenvalue.

Besides the renormalisation study, which is going to be described in the following sections, we evaluate the integrated electronic density of states (DOS) $D(E)$ also by means of the negative eigenvalue method (Dean 1972, Ma *et al* 1986) for a finite chain consisting of 15 000 atoms described by the same Hamiltonian (3). The results of numerical simulation will be used to check the accuracy of renormalisation calculations.

Before concluding this section, we note a few simple facts in the structure of a Thue–Morse chain shown in figure 1, which will be useful later. If we switch off the long bonds (setting $T_L = 0$) in figure 1, the whole chain breaks into a sequence of isolated monatomic, diatomic and triatomic molecules. Let N_M, N_D and N_T be the corresponding numbers of these molecules in a chain of total number of atoms N. Then obviously,

$$N_M + 2N_D + 3N_T = N \tag{7}$$

$$N_D + 2N_T = N_S \tag{8}$$

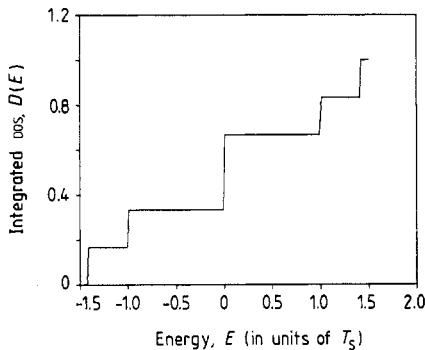$$N_S = N_L = \tfrac{1}{2}N \tag{9}$$

where N_L and N_S are the number of long and short bonds, respectively. Equations (7)–(9) imply $N_M = N_T$. Moreover, closer examination of the generation rule tells us $N_M = N_D$. Hence

$$N_M = N_D = N_T = \tfrac{1}{6}N. \tag{10}$$

By switching off the long bonds ($T_L = 0$), there are only five energy eigenvalues arising from the monatomic, diatomic and triatomic molecules, respectively, $E =$

Table 1. Energy levels in the zeroth approximation, $T_L = 0$.

Levels (in units T_S)	DOS $\rho(E)$	Integrated DOS $D(E) = \int_{-\infty}^{E} \rho(E')\, dE'$
-2	$\frac{1}{6}$	$\frac{1}{6}$
-1	$\frac{1}{6}$	$\frac{1}{3}$
0	$\frac{1}{3}$	$\frac{2}{3}$
$+1$	$\frac{1}{6}$	$\frac{5}{6}$
$+2$	$\frac{1}{6}$	1

Figure 2. The integrated DOS $D(E)$ versus energy E curve in the zeroth approximation with $T_L = 0$.

$-\sqrt{2}$, -1, 0 (doubly degenerate), 1 and $\sqrt{2}$ (in units of T_S). In view of (10), we list in table 1 the levels as well as the corresponding DOS $\rho(E)$ and integrated DOS $D(E) = \int_{-\infty}^{E}\rho(E')\, dE'$ providing the basis from which we shall begin our renormalisation calculation in the case $T_L \neq 0$ but $|T_L/T_S| \ll 1$. The integrated DOS $D(E)$ is also illustrated in figure 2, where we can see the principal step structure in the $D(E)$ versus E curve. More detailed fine structures are going to be explored in the following two sections. Section 2 discusses first the level $E = 0$ whereas § 3 deals with the other four levels. Some discussions are given in § 4.

2. Renormalisation analysis of electronic structure: level $E = 0$

Switching on a small T_L, such that $|T_L/T_S| \ll 1$, introduces two main effects on the levels listed in table 1, namely level split and level shift. We begin now to analyse these effects on each of the levels in table 1 separately, by means of a renormalisation procedure.

In the zeroth approximation ($T_L = 0$) $E = 0$ has a higher ($N/3$-fold) degeneracy than any other level in table 1 and/or figure 2. We would like to tackle this level first. In the zeroth approximation, it originates from the energy eigenvalue of either monatomic or triatomic molecules. With switching on of T_L, each molecule is coupled to its nearest neighbouring molecules at a strength T_L. We need to calculate the effective coupling strength between two nearest-neighbour molecules in eigenstates belonging to the same level $E = 0$. There are, thus, two possible cases, as one can see from figure 1. In the first case a monatomic molecule is coupled directly through a long bond T_L to a triatomic
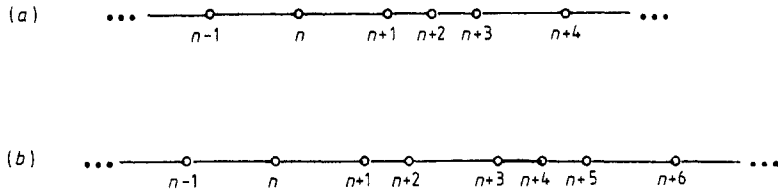
Figure 3. (*a*) A monatomic molecule (*n*) coupled to a triatomic molecule (*n* + 1, *n* + 2, *n* + 3) through a direct long bond. (*b*) A monatomic molecule (*n*) coupled to a triatomic molecule (*n* + 3, *n* + 4, *n* + 5) indirectly through two long bonds and a diatomic molecule (*n* + 1, *n* + 2).

molecule (figure 3(*a*)) while in the second case it is coupled indirectly through two long bonds T_L and a diatomic molecule (figure 3(*b*)). These are the only two possible configurations since monatomic and triatomic molecules always occur alternately along the chain in figure 1.

Consider the case of figure 3(*a*) first. We write relevant Schrödinger equations as

$$T_L |n - 1\rangle + T_L |n + 1\rangle = E|n\rangle$$

$$T_L |n\rangle + T_S |n + 2\rangle = E|n + 1\rangle \tag{11}$$

$$T_S |n + 1\rangle + T_S |n + 3\rangle = E|n + 2\rangle.$$

The eigenstates of a triatomic molecule are

$$|\sqrt{2}\rangle = (1/2)(|n + 1\rangle + \sqrt{2}|n + 2\rangle + |n + 3\rangle)$$

$$|0\rangle = (\sqrt{2}/2)(|n + 1\rangle - |n + 3\rangle) \tag{12}$$

$$|-\sqrt{2}\rangle = (1/2)(|n + 1\rangle - \sqrt{2}|n + 2\rangle + |n + 3\rangle)$$

corresponding respectively to the energy eigenvalues $\sqrt{2}$, 0 and $-\sqrt{2}$. Expressing $|n + 1\rangle$, $|n + 2\rangle$ and $|n + 3\rangle$ in terms of $|\pm\sqrt{2}\rangle$ and $|0\rangle$, and substituting into the last two equations of (11) with $|n + 2\rangle$ eliminated, we have by combining the result with the first equation of (11)

$$T_L |n - 1\rangle + \left(\frac{\sqrt{2}}{2} T_L + \frac{\sqrt{2}E^2 T_L}{4T_S^2 - E^2}\right)|0\rangle = E\left(1 + \frac{T_L^2}{2T_S^2 - E^2}\right)|n\rangle \tag{13}$$

which can be simplified in view of $E \simeq 0$, $|T_L/T_S| \ll 1$, into

$$T_L |n - 1\rangle + (\sqrt{2}/2)T_L |0\rangle = E|n\rangle. \tag{14}$$

Therefore, the effective coupling strength between a monatomic molecule and a triatomic molecule in the $|0\rangle$ state is, in this case,

$$T_S' = (\sqrt{2}/2)T_L. \tag{15}$$

In the case of figure 3(*b*), rearrangement of the Schrödinger equations

Table 2. First-order splitting of level $E = 0$ in table 1 with $T_L = 0.1T_S$.

Levels (in units T_S)		Integrated DOS $D(E)$	
Calculated	Numerical simulation	Calculated	Numerical simulation
$-\sqrt{2}T_S' = -T_L = -0.1$	-0.1000	$\frac{1}{3} \times \frac{1}{4} + \frac{1}{3}^a = \frac{5}{12} = 0.4167$	0.4167
0	0.0000	$\frac{1}{3} \times \frac{1}{2} + \frac{5}{12} = \frac{7}{12} = 0.5833$	0.5833
$\sqrt{2}T_S' = T_L = 0.1$	0.1000	$\frac{1}{3} \times \frac{1}{4} + \frac{7}{12} = \frac{8}{12} = 0.6667$	0.6667

^{a} This is the value of $D(E)$ in the second line in table 1.

$$T_L|n - 1\rangle + T_L|n + 1\rangle = E|n\rangle$$

$$T_L|n\rangle + T_S|n + 2\rangle = E|n + 1\rangle$$

$$T_S|n + 1\rangle + T_L|n + 3\rangle = E|n + 2\rangle \tag{16}$$

$$T_L|n + 2\rangle + T_S|n + 4\rangle = E|n + 3\rangle$$

$$T_S|n + 3\rangle + T_S|n + 5\rangle = E|n + 4\rangle$$

in a like manner yields

$$T_L|n - 1\rangle - \frac{\sqrt{2}}{2}\frac{T_L^2}{T_S}|0\rangle = E|n\rangle \tag{17}$$

so that the effective coupling strength is, in the second case,

$$T_L' = -(\sqrt{2}/2)/T_L^2/T_S \qquad |T_L'/T_S'| = |T_L/T_S| \ll 1. \tag{18}$$

Regarding the monatomic and triatomic molecules as 'equivalent atoms' coupled via T_S' and/or T_L', we obtain the following transformed sequence:

$$L'S'S'L'L'L'S'S'L'S'S'L'S'S'L'L'L'S'S'L'L'L'S'S' \ldots \tag{19}$$

implying a transformed atomic chain shown in figure 4. If we switch off all bonds L', we obtain a collection of 'monatomic' and 'triatomic molecules' in equal numbers $N_M' = N_T' = \frac{1}{4}N'$, N' being the total number of 'equivalent atoms'. We thus obtain split levels and first-order steps in the $D(E)$ versus E curve summarised in table 2. Along with the results of renormalisation calculations we have also listed in table 2 results of numerical simulation with 15 000 atoms. The agreement is entirely satisfactory. The
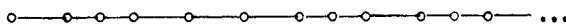

Figure 4. The equivalent atomic chain in accordance with the renormalisation transformed sequence (19).
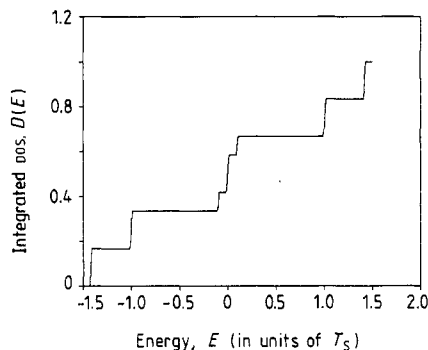
Figure 5. The $D(E)$ versus E curve in the neighbourhood of $E = 0$ in the first approximation showing fine structure in comparison with figure 2 ($T_L/T_S = 0.1$).
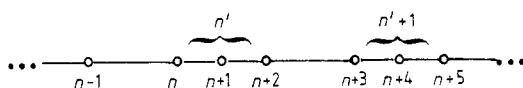

Figure 6. Two triatomic molecules $n' = (n, n + 1, n + 2)$ and $n' + 1 = (n + 3, n + 4, n + 5)$ coupled directly via a long bond.

first-order steps are shown in the central part of figure 5, too. We shall see later that the zeroth-order levels $E = \pm T_S$ and $\pm\sqrt{2}T_S$ do not split at the order $|T_L/T_S|$.

We can pursue the renormalisation calculation further to the second approximation. When T_L' is switched on in figure 4, there are three different ways of coupling between 'molecules' with energy eigenvalue $E = 0$, namely coupling via a long bond (i) between 'monatomic molecules' as two nearest neighbours, (ii) between a 'monatomic molecule' and a 'triatomic molecule' as nearest neighbours and (iii) between two 'triatomic molecules'. In the third case, for example, we obtain from Schrödinger's equations for the transformed chain (figure 6)

$$T_L'|n - 1\rangle + T_S'|n + 1\rangle = E|n\rangle$$

$$T_S'|n\rangle + T_S'|n + 2\rangle = E|n + 1\rangle$$

$$T_S'|n + 1\rangle + T_L'|n + 3\rangle = E|n + 2\rangle \qquad (20)$$

$$T_L'|n + 2\rangle + T_S'|n + 4\rangle = E|n + 3\rangle$$

$$T_S'|n + 3\rangle + T_S|n + 5\rangle = E\rangle|n + 4\rangle$$

the reduced relation

$$(\sqrt{2}/2)T_L'|n - 1\rangle - \tfrac{1}{2}T_L'|0, n' + 1\rangle = E|0, n'\rangle \qquad (21)$$

where $|0, n'\rangle$ denotes the $E = 0$ eigenstate of the n'th 'triatomic molecule'. So the effective coupling strength is, in this case, $-\tfrac{1}{2}T_L'$. It can be visualised that the effective coupling strengths in the first and second cases are, respectively, T_L' and $(\sqrt{2}/2)T_L'$. Since in all three cases the effective coupling strengths have the same order of magnitude, the situation is very close to the case of a one-dimensional periodic chain of atoms with $T_L = T_S$, implying that the level splitting is not so apparent, or in other words the $D(E)$ versus E curve in the neighbourhood of $E = 0$ is quite smooth as in the periodic case
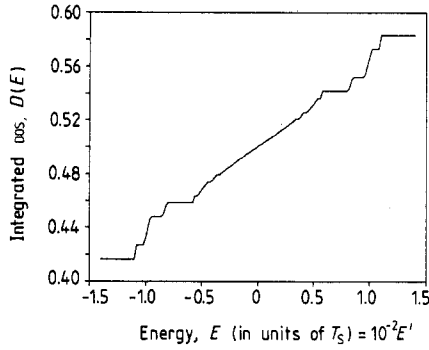
Figure 7. The $D(E)$ versus E curve showing an almost continuous spectrum in the neighbourhood of $E = 0$ in the second approximation.
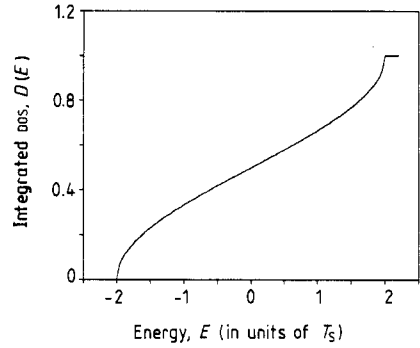

Figure 8. The $D(E)$ versus E curve of a periodic chain with $|T_L/T_S| = 1$ showing a continuous spectrum.

(compare figures 7 and 8). It is possible to estimate the width of the 'continuous spectrum'. Assuming the coupling strengths in all three cases to take the geometrical mean value $(\sqrt{2}/2)T'_L = \frac{1}{2}T'^2_L T'^{-1}_S$ and considering the transformed chain as a periodic one, we obtain a half-bandwidth $2 \times \frac{1}{2}T'^2_L T'^{-1}_S = 0.01$. In comparison, numerical simulation yields a value 0.0109.

Consider next the splitting of the level $\sqrt{2}T'_S = T_L = 0.1$ in table 2, which corresponds to the state $|\sqrt{2}\rangle$ of an 'equivalent' 'triatomic' molecule. From figure 4 we see there are two coupling schemes between two 'triatomic molecules', namely (i) via a long bond and (ii) via three long bonds and two 'monatomic molecules'. In the first case, we obtain from Schrödinger's equations for the transformed chain, equation (20),

$$\tfrac{1}{2}T'_L |n - 1\rangle + \tfrac{1}{4}T'_L |\sqrt{2}, n' + 1\rangle = \left(E - \sqrt{2}T'_S - \frac{\sqrt{2}T'^2_L}{8T'_S} \right) |\sqrt{2}, n'\rangle \quad (22)$$

where $|\sqrt{2}, n'\rangle$ denotes the $E = \sqrt{2}T'_S = T_L$ eigenstate of the n'th 'triatomic molecules'. We see, therefore, that the effective coupling strength between $|\sqrt{2}, n'\rangle$ and $|\sqrt{2}, n' + 1\rangle$ is $T''_S = \tfrac{1}{4}T'_L = (\sqrt{2}/8)T'^2_L T'^{-1}_S$. Besides, there is also a shift $\Delta E = (\sqrt{2}/8)T'^2_L T'^{-1}_S = \tfrac{1}{8}T'^3_L T'^{-2}_S$ in the original level $E = \sqrt{2}T'_S = T_L$. A similar analysis yields for the second coupling scheme an effective coupling strength between $|\sqrt{2}, n'\rangle$ and $|\sqrt{2}, n' + 1\rangle$, $T''_L = \tfrac{1}{8}T'^3_L T'^{-2}_S$.

Replacing the system by effective bonds T''_S and T''_L connecting 'triatomic molecules' as reduced single particles, we obtain for the transformed chain after renormalisation a second time exactly the sequence (19) or equivalently figure 4. Since $|T''_L/T''_S| \ll 1$, deleting the long bonds, we again obtain a collection of 'triatomic' molecules. Owing to its smallness in order of magnitude, $\Delta E = \tfrac{1}{8}T'^3_L T'^{-2}_S$ can also be neglected. We thus obtain the second-order splitting of the first-order level $E = \sqrt{2}T'_S = T_L$ into three:

$$E = \begin{cases} \sqrt{2}T'_S - \sqrt{2}T''_S = T_L - \tfrac{1}{4}T'^2_L T'^{-1}_S & \rho(E) = \tfrac{1}{4} \\ \sqrt{2}T'_S = T_L & \rho(E) = \tfrac{1}{2} \\ \sqrt{2}T'_S + \sqrt{2}T''_S = T_L + \tfrac{1}{4}T'^2_L T'^{-1}_S & \rho(E) = \tfrac{1}{4}. \end{cases} \quad (23)$$

A comparison with numerical simulation is given in table 3. Equations (23) and (24)

Table 3. Second-order splitting of the first-order level $E = \sqrt{2}T'_S = T_L$ in table 2 (adopting $T_L = 0.1T_S$).

Levels (in units T_S)		Integrated DOS $D(E)$	
Calculated	Numerical simulation	Calculated	Numerical simulation
$T_L - \frac{1}{4}T_L^2 T_S^{-1} = 0.0975$	0.0975	$\frac{7}{12}^a + \frac{1}{12} \times \frac{1}{4} = \frac{29}{48} = 0.6042$	0.6042
$T_L = 0.1$	0.1000	$\frac{29}{48} + \frac{1}{12} \times \frac{1}{2} = \frac{31}{48} = 0.6458$	0.6459
$T_L + \frac{1}{4}T_L^2 T_S^{-1} = 0.1025$	0.1022	$\frac{31}{48} + \frac{1}{12} \times \frac{1}{4} = \frac{2}{3} = 0.6667$	0.6667

^{a} This is the value of $D(E)$ in the second line in table 2.

determine the second-order fine structures on the $D(E)$ versus E curve in the relevant energy range.

The level $E = -\sqrt{2}T'_S = -T_L$ is in exactly symmetrical situation and needs no more discussion.

3. Renormalisation analysis of electronic structure: levels $E = \pm T_S$ and $\pm\sqrt{2}T_S$

Consider, for the moment, the level $E = T_S$, which corresponds to one of the two eigenstates of a diatomic molecule. Examination of figure 1 tells us that there are four different schemes of couplings between diatomic molecules shown in figures 9(a)–(d). In the case of figure 9(a), we derive from the Schrödinger equations

$$
\begin{aligned}
T_L|n-1\rangle + T_S|n+1\rangle &= E|n\rangle \\
T_S|n\rangle + T_L|n+2\rangle &= E|n+1\rangle \\
T_L|n+1\rangle + T_L|n+3\rangle &= E|n+2\rangle \\
T_L|n+2\rangle + T_S|n+4\rangle &= E|n+3\rangle
\end{aligned}
\tag{24}
$$

the relation

$$
\frac{\sqrt{2}}{2} T_L|n-1\rangle + \frac{T_L^2}{2T_S}|+,n'\rangle = \left(E - T_S - \frac{T_L^2}{2T_S}\right)|+,n\rangle
\tag{25}
$$

where $|\pm, n'\rangle = (\sqrt{2}/2)(|n\rangle \pm |n+1\rangle)$ are the two eigenstates corresponding to the eigenenergies $\pm T_S$ of the n'th diatomic molecule composed of the atoms n and $n+1$. Equation (25) tells us that the effective coupling strength is, in this case, $\frac{1}{2}T_L^2/T_S$ with a corresponding level shift $\Delta E_a = \frac{1}{2}T_L^2 T_S^{-1}$. In the cases of figures 9(b)–(d), one obtains effective coupling strengths $\frac{1}{2}T_L^2 T_S^{-1}$, $-\frac{1}{2}T_L^4 T_S^{-3}$ and $\frac{1}{2}T_L^4 T_S^{-3}$ and level shifts 0, $\Delta E_c = \frac{1}{2}T_L^2 T_S^{-1} = \Delta E_a \equiv \Delta E$ and 0, respectively. Denoting accordingly the bonds of different strengths by a, b, c and d, they appear along the chain in the following order:

$$cbadcdabcbadabcdc \ldots$$

Note that (c and/or a) and (b and/or d) always occur alternately, so that each diatomic molecule is connected to neighbouring ones on one and only one side by either an a or a c bond, inducing a shift $\Delta E = -\frac{1}{2}T_L^2 T_S^{-1}$ in the energy level of every molecule.
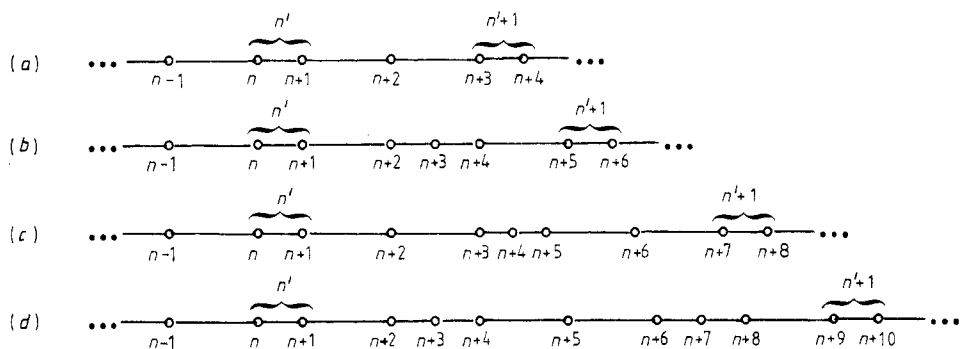
Figure 9. (*a*) Two diatomic molecules $n' = (n, n + 1)$ and $n' + 1 = (n + 3, n + 4)$ coupled via two long bonds and a monatomic molecule $n + 2$. (*b*) Two diatomic molecules $n' = (n, n + 1)$ and $n' + 1 = (n + 5, n + 6)$ coupled via two long bonds and a triatomic molecule $(n + 2, n + 3, n + 4)$. (*c*) Two diatomic molecules $n' = (n, n + 1)$ and $n' + 1 = (n + 7, n + 8)$ coupled via four long bonds, two monatomic $(n + 2, n + 6)$ and one triatomic $(n + 3, n + 4, n + 5)$ molecules. (*d*) Two diatomic molecules $n' = (n, n + 1)$ and $n' + 1 = (n + 9, n + 10)$ coupled via four long bonds, one monatomic $(n + 5)$ and two triatomic $((n + 2, n + 3, n + 4), (n + 6, n + 7, n = 8))$ molecules.

Table 4. Splitting of zeroth-order level $E = T_S$ in table 1 (adopting $T_L = 0.1 T_S$).

Levels (in units T_S)		Integrated DOS $D(E)$	
Calculated	Numerical simulation	Calculated	Numerical simulation
$T_S + (1 - \sqrt{2}/2) T_L^2 T_S^{-1} = 0.9979$	0.9979	$\frac{2}{3}^a + \frac{1}{6} \times \frac{1}{4} = \frac{17}{24} = 0.7083$	0.7083
$T_S + \frac{1}{2} T_L^2 T_S^{-1} = 1.0050$	1.0050	$\frac{17}{24} + \frac{1}{6} \times \frac{1}{2} = \frac{19}{24} = 0.7917$	0.7917
$T_S + (1 + \sqrt{2}/2) T_L^2 T_S^{-1} = 1.0121$	1.0120	$\frac{19}{24} + \frac{1}{6} \times \frac{1}{4} = \frac{5}{6} = 0.8333$	0.8333

^{a} This is the value of $D(E)$ in the third line in table 1.

The bonds c and d have strength $|T_L'| = \frac{1}{2} T_L^4 T_S^{-3}$, weaker in order of magnitude in comparison with bonds a and b of strengths $T_S' = \frac{1}{2} T_L^2 T_S^{-1}$. Replacing a and b with S and c and d with L, we have once again the sequence (19). Regarding each diatomic molecule as a single entity, we have once again the transformed chain of figure 4. Deletion of T_L' again gives a collection of monatomic and triatomic molecules, whereby we obtain the fine structure of the $E = T_S$ levels as

$$T_S + \Delta E - \sqrt{2} T_S' = T_S + \frac{1}{2} T_L^2 T_S^{-1} - \frac{\sqrt{2}}{2} T_L^2 T_S^{-1} = T_S + \frac{1 - \sqrt{2}}{2} T_L^2 T_S^{-1} \qquad \rho(E) = \tfrac{1}{4}$$

$$T_S + \Delta E = T_S + \frac{1}{2} T_L^2 T_S^{-1} \qquad\qquad\qquad\qquad\qquad\qquad \rho(E) = \tfrac{1}{2} \quad (26)$$

$$T_S + \Delta E + \sqrt{2} T_S' = T_S + \frac{1}{2} T_L^2 T_S^{-1} + \frac{\sqrt{2}}{2} T_L^2 T_S^{-1} = T_S + \frac{1 + \sqrt{2}}{2} T_L^2 T_S^{-1} \qquad \rho(E) = \tfrac{1}{4}.$$

Comparison with numerical simulation is given in table 4. We note that the energy differences between the split levels are already of the order of $T_L^2 T_S^{-1}$, so that, as we
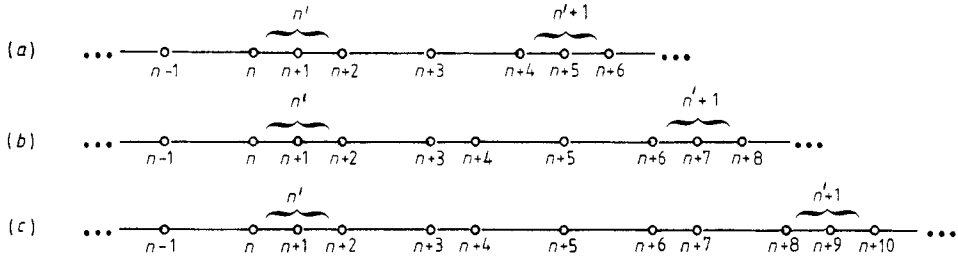
Figure 10. (*a*) Two triatomic molecules $n' = (n, n + 1, n + 2)$ and $n' + 1 = (n + 4, n + 5, n + 6)$ coupled via two long bonds and a monatomic molecule $(n + 3)$. (*b*) Two triatomic molecules $n' = (n, n + 1, n + 2)$ and $n' + 1 = (n + 6, n + 7, n + 8)$ coupled via three long bonds, a diatomic $(n = 3, n + 4)$ and a monatomic $(n + 5)$ molecule. (*c*) Two triatomic molecules $n' = (n, n + 1, n + 2)$ and $n' + 1 = (n + 8, n + 9, n + 10)$ coupled via four long bonds, a monatomic $(n + 5)$ and two diatomic $((n + 3, n + 4), (n + 6, n + 7))$ molecules.

mentioned before, there is no first-order splitting of the level $E = T_S$. It is hardly necessary to say that, by symmetry, the analysis applies to the level $E = -T_S$, too.

Let us turn lastly to the level $E = \sqrt{2}T_S$ in the zeroth approximation. Investigation of figure 1 shows that there are three different coupling schemes between two triatomic molecules, shown separately in figures 10(*a*)–(*c*). In the case of figure 10(*a*), starting from the Schrödinger equations

$$T_L |n - 1\rangle + T_S |n + 1\rangle = E|n\rangle$$

$$T_S |n\rangle + T_S |n + 2\rangle = E|n + 1\rangle$$

$$T_S |n + 1\rangle + T_L |n + 3\rangle = E|n + 2\rangle$$

$$T_L |n + 2\rangle + T_L |n + 4\rangle = E|n + 3\rangle \tag{27}$$

$$T_L |n + 3\rangle + T_S |n + 5\rangle = E|n + 4\rangle$$

$$T_S |n + 4\rangle + T_S |n + 6\rangle = E|n + 5\rangle$$

substitution for $|n\rangle$, $|n + 1\rangle$, $|n + 2\rangle$ and $|n + 4\rangle$, $|n + 5\rangle$, $|n + 6\rangle$ in terms of the triatomic molecular states $|\pm\sqrt{2}, n'\rangle$, $|0, n'\rangle$ and $|\pm\sqrt{2}, n' + 1\rangle$, $|0, n' + 1\rangle$, respectively, elimination of $|n + 3\rangle$, $|-\sqrt{2}, n'\rangle$, $|0, n'\rangle$, $|-\sqrt{2}, n' + 1\rangle$ and $|0, n' + 1\rangle$, and neglect of higher-order terms lead to

$$\tfrac{1}{2}T_L |n - 1\rangle + \frac{\sqrt{2}}{8} T_L^2 T_S^{-1} |\sqrt{2}, n' + 1\rangle = \left(E - \sqrt{2}T_S - \frac{\sqrt{2}}{8} T_L^2 T_S^{-1} \right) |\sqrt{2}, n'\rangle. \tag{28}$$

Hence, the effective coupling strength between the states $|\sqrt{2}, n'\rangle$ and $|\sqrt{2}, n' + 1\rangle$ in case (*a*) in figure 10 is

$$T_S' = (\sqrt{2}/8)T_L^2 T_S^{-1} \qquad \text{along with a level shift} \qquad \Delta E_a = (\sqrt{2}/8)T_L^2 T_S^{-1}. \tag{29}$$

A similar analysis yields, in the cases of figures 10(*b*) and (*c*), respectively, for the effective coupling strengths and level shifts

$$T_{L1}' = (\sqrt{2}/16)T_L^3 T_S^{-2} \qquad \Delta E_b = \Delta E_a \equiv \Delta E$$

$$T_{L2}' = (\sqrt{2}/32)T_L^4 T_S^{-3} \qquad \Delta E_c = \tfrac{1}{2}\Delta E. \tag{30}$$

Here T_{L1}' and T_{L2}' are of higher orders of magnitude than T_S' and can be omitted.
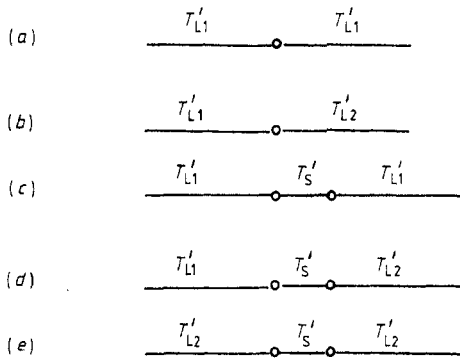
Figure 11. (a) An equivalent monatomic molecule coupled at both ends via renormalised bonds of strength T'_{L1}. (b) An equivalent monatomic molecule coupled at one end via a renormalised bond of strength T'_{L1} and at the other end via a renormalised bond of strength T'_{L2}. (c) An equivalent diatomic molecule coupled at both ends via renormalised bonds of strength T'_{L1}. (d) An equivalent diatomic molecule coupled at one end via a renormalised bond of strength T'_{L1} and at the other end via a renormalised bond of strength T'_{L2}. (e) An equivalent diatomic molecule coupled at both ends via renormalised bonds of strength T'_{L2}.

However, ΔE_a, ΔE_b and ΔE_c have the same order of magnitude as T'_S, and must not be ignored.

Regarding the triatomic molecules in the state $|\sqrt{2}\rangle$ as equivalent single atoms with appropriate level shifts coupled through the effective bond T'_S, equation (29) (with T'_{L1} and T'_{L2} switched off), we are left with a collection of monatomic and diatomic molecules. There is complexity in the different surroundings of the atoms, leading to different level shifts, as shown in figures 11(a)–(e), where all possible cases have been enumerated. In view of the level-shift contributions given in (29) and (30), we have in cases (a) and (b), the split levels

$$E_a = \sqrt{2}T_S + 2(\sqrt{2}/8)T_L^2 T_S^{-1} = \sqrt{2}T_S + (\sqrt{2}/4)T_L^2 T_S^{-1} \qquad \rho(E) = \tfrac{1}{24} \qquad (31)$$

$$E_b = \sqrt{2}T_S + (\sqrt{2}/8)T_L^2 T_S^{-1} + (\sqrt{2}/16)T_L^2 T_S^{-1}$$
$$= \sqrt{2}T_S + (3\sqrt{2}/16)T_L^2 T_S^{-1} \qquad \rho(E) = \tfrac{1}{24}. \qquad (32)$$

It is also easily seen that in the cases (c) and (e),

$$E_{c\pm} = \sqrt{2}T_S + 2(\sqrt{2}/8)T_L^2 T_S^{-1} \pm (\sqrt{2}/8)T_L^2 T_S^{-1}$$

$$= \sqrt{2}T_S + \begin{cases} (3\sqrt{2}/8)T_L^2 T_S^{-1} \\ (\sqrt{2}/8)T_L^2 T_S^{-1} \end{cases} \qquad \rho(E) = \tfrac{1}{96} \qquad (33)$$

$$E_{e\pm} = \sqrt{2}T_S + (\sqrt{2}/8)T_L^2 T_S^{-1} + (\sqrt{2}/16)T_L^2 T_S^{-1} \pm (\sqrt{2}/8)T_L^2 T_S^{-1}$$

$$= \sqrt{2}T_S + \begin{cases} (5\sqrt{2}/16)T_L^2 T_S^{-1} \\ (\sqrt{2}/16)T_L^2 T_S^{-1} \end{cases} \qquad \rho(E) = \tfrac{1}{96}. \qquad (34)$$

In case (d), the energy eigenvalues of the split levels can be found by solving the following secular equation:

$$\begin{vmatrix} (3\sqrt{2}/16)T_L^2 T_S^{-1} - (E - \sqrt{2}T_S) & (\sqrt{2}/8)T_L^2 T_S^{-1} \\ (\sqrt{2}/8)T_L^2 T_S^{-1} & (\sqrt{2}/4)T_L^2 T_S^{-1} - (E - \sqrt{2}T_S) \end{vmatrix} = 0 \qquad (35)$$

namely,

$$E_{d\pm} = \sqrt{2}T_S + \frac{7 \pm \sqrt{17}}{16\sqrt{2}} T_L^2 T_S^{-1} \qquad \rho(E) = \tfrac{1}{48}. \qquad (36)$$

Table 5. Splitting of zeroth-order level $E = \sqrt{2}T_S$ in table 1 (adopting $T_L = 0.1T_S$).

Levels (in units T_S)		Integrated DOS $D(E)$	
Calculated	Numerical simulation	Calculated	Numerical simulation
$E_{e-} = 1.415$		$\frac{5}{8}^a + \frac{1}{96} = \frac{27}{32} = 0.8438$	
$E_{c-} = 1.415$	1.418	$\frac{27}{32} + \frac{1}{96} = \frac{41}{48} = 0.8542$	0.8542
$E_{d-} = 1.416$		$\frac{41}{48} + \frac{1}{48} = \frac{7}{8} = 0.8750$	
$E_b = 1.417$	1.419	$\frac{7}{8} + \frac{1}{24} = \frac{11}{12} = 0.9167$	0.9167
$E_a = 1.418$	1.421	$\frac{11}{12} + \frac{1}{24} = \frac{23}{24} = 0.9583$	0.9583
$E_{e+} = 1.419$		$\frac{23}{24} + \frac{1}{96} = \frac{31}{32} = 0.9688$	
$E_{d+} = 1.419$		$\frac{31}{32} + \frac{1}{48} = \frac{95}{96} = 0.9896$	
$E_{c+} = 1.420$	1.421	$\frac{95}{96} + \frac{1}{96} = 1$	1.0000

[a] This is the value of $D(E)$ in the fourth line in table 1.

Thus the $E = \sqrt{2}T_S$ level splits up to the order $(T_L^2 T_S^{-1})$ into eight given in equations (31)–(34) and (36). Numerical results in the case $T_L/T_S = 0.1$ are given in table 5, where owing to smallness in level separation and limitation in the accuracy of numerical simulation working with 15 000 atoms, computer simulation gives only the levels E_{c-}, E_b, E_a and E_{c+} and is unable to differentiate all other sublevels in the fine structure of $E = \sqrt{2}T_S$. Note that there is also a source of error in the numerical values of calculated levels, for we have assumed consistently $|T_L/T_S| \ll 1$, whereas we put $T_L = 0.1T_S$ in obtaining the numbers in the first column in table 5. We remark again that the above analysis applies to the zeroth-order level $E = -\sqrt{2}T_S$, too.

4. Discussion

We have studied analytically the electronic structure of a Thue–Morse aperiodic chain in the $|T_L/T_S| \ll 1$ case by means of a renormalisation procedure. The results agree very satisfactorily with numerical simulation. From our experience on the feasibility and effectiveness of the method in the case of a Fibonacci quasi-crystal (Ma and Tsai 1988) and in the present case, we speculate that the method is not limited to one-dimensional problems. In principle, it should have the potentiality to be generalised and modified to solve two- and three-dimensional problems like the Penrose lattice or real quasi-crystals. The algebra might be much more involved and might become cumbersome for, or even beyond the possibility of, manual calculations. However, higher-dimensional problems might still be tractable with the help of the computer algebra. Developments in this direction are greatly expected by the importance of studying realistic quasi-crystals.

In the above calculations, we have assumed $e_M = e_D = e_T$. It is not difficult to treat the case of unequal e by the same method. The main feature in the case of unequal e is the loss of antisymmetry of the $D(E)$ versus E curve with respect to $E = 0$.

As expected by Riklund *et al* (1987), the Thue–Morse chain has properties lying midway between a Fibonacci quasi-crystal and a periodic chain. The above analysis shows that the electronic spectrum of a Thue–Morse chain consists of parts displaying Cantor structure characteristic of aperiodic systems as well as a continuous band very similar in nature to that of a periodic chain (figure 7). Our analytical discussions do show a tendency of the Thue–Morse chain to approach a periodic system.

An important difference of the Thue–Morse aperiodic chain from the Fibonacci quasi-crystal is the absence of simple self-similarity in either the geometrical structure or the step structure in the $D(E)$ versus E curve. Our previous work (Ma and Tsai 1988) on the Fibonacci problem utilised greatly the self-similarity. We were thus able to derive the fine structure in the electronic spectrum to indefinitely higher and higher orders. Indeed, the results contained in table 1 of Ma and Tsai (1988) and continuation to all higher orders are exact and independent of the condition $|T_L/T_S| \ll 1$ repeatedly used in the analysis. We expect that it should be possible to derive table 1 of Ma and Tsai (1988) on much more general grounds, relying mainly on the self-similarity. In the case of a Thue–Morse chain, absence of simple self-similarity limits results of the present analysis to be valid only when $|T_L/T_S| \ll 1$. Furthermore, extension of calculations to orders higher than second becomes difficult for lack of a simple guiding rule.

Acknowledgment

References

Allouche J P *et al* 1966 *C.R. Acad. Sci., Paris* **302** 1135
Axel F, Allouche J P, Kleman M, Mendes-France M and Peyriere J 1986 *J. Physique Coll.* **C3** 181
Cheng Z, Savit R and Merlin R 1988 *Phys. Rev.* B **37** 4375
Dean P 1972 *Rev. Mod. Phys.* **44** 127
Garg A 1988 *Phys. Rev.* B **37** 10003
Ma H R and Tsai C H 1988 *J. Phys. C: Solid State Phys.* **21** 4311
Ma H R, Xu Y and Tsai C H 1986 *J. Phys. C: Solid State Phys.* **19** L823
Niu Q and Nori F 1986 *Phys. Rev. Lett.* **57** 2057
Riklund R, Severin M and Liu Y 1987 *J. Mod. Phys.* B **1** 121